 doi:10.20944/preprints202306.1270.v1

Article

Optimal Design of Bubble Deck Concrete Slabs: Serviceability Limit State

Tomasz Gajewski [1], Natalia Staszak[2] and Tomasz Garbowski [3,*]

[1] Institute of Structural Analysis, Poznan University of Technology, Piotrowo 5, 60-965 Poznań, Poland; tomasz.gajewski@put.poznan.pl
[2] Doctoral School, Poznan University of Life Sciences, Wojska Polskiego 28, 60-637 Poznań, Poland; natalia.staszak@up.poznan.pl
[3] Department of Biosystems Engineering, Poznan University of Life Sciences, Wojska Polskiego 50, 60-627 Poznań, Poland
* Correspondence: tomasz.garbowski@up.poznan.pl

Abstract: In engineering practice, one can often encounter issues related to optimization where the goal is to minimize material consumption, minimize stresses or deflections of the structure. In most cases, these issues are addressed with finite element analysis software and simple optimization algorithms. However, in the case of optimization of certain structures, it is not co straightforward. An example of such constructions are bubble deck ceilings, where in order to reduce the dead weight, air cavities are used, which are regularly arranged over the entire surface of the ceiling. In the case of these slabs, the flexural stiffness is not constant in all its cross-sections, which means that the use of structural finite elements (plate or shell) for static calculations is not possible, and therefore the optimization process becomes more difficult. The paper presents a minimization procedure of the weight of bubble deck slabs using numerical homogenization and sequential quadratic programming with constraints. Homogenization allows to determine the effective stiffnesses of the floor, which in the next step are sequentially corrected by changing the geometrical parameters of the floor and voids in order to achieve the assumed deflection. The presented procedure allows to minimize the use of material in a quick and effective way by automatically determining the optimal parameters describing the geometry of the bubble deck floor cross-section.

Keywords: lightweight structures; bubble deck concrete slabs; numerical homogenization; weight minimization; sequential quadratic programming;

1. Introduction

Over the last few decades, concrete structures, in particular prefabricated reinforced concrete structures, have gained popularity and found wide application in many construction sectors around the world [1]. They are used not only in industrial, commercial or residential facilities, but also in the infrastructural constructions. Prefabricated reinforced concrete elements, among others, mainly include: columns, foundation footings and retaining walls, as well as, prefabricated walls with window and door openings. However, the most commonly used prefabricated concrete elements are girders and floor slabs [2].

This type of construction has numerous of advantages, including: (a) saving formwork, (b) high durability and resistance of the structure, (c) high strength, (d) short construction time, (e) quality standard and (f) reducing the amount of work on construction sites. In addition, prefabricated structures can be shaped in many ways using modern technologies and adapted to local conditions that occur in the designed facilities. Moreover, during the production stage, it is possible to make cuts and openings which allow carry out installation, e.g. pipes or cables after mounting the element at the site. It is extremely important to plan and anticipate all required openings already at the design stage.

 doi:10.20944/preprints202306.1270.v1

On the other hand, prefabricated elements have also disadvantages. One of the main disadvantages is their cost, which consists of production, transport and the need for cranes for their assembly [3]. However, the recent is not problem, because on large construction sites, in which such structures are used, heavy equipment is available to unload and assemble them.

The main idea of the floor technology has remained unchanged in its general concept for years. Each type of ceiling should meet specific requirements that determine the selection of the appropriate structure and technology [4]. Technical requirements including thermal and acoustic insulation, adequate strength, stiffness, fire resistance and durability have the greatest impact. Another important aspect is economic requirements, which include minimization of costs during construction and the project design stage. In the case of large spans between supports, prefabricated floors are used. The basic types of such floors are solid slabs, filigree slabs, multi-hole slabs and TT double-rib slabs [5]. In such structures, an important aspect is to increase the span and at the same time reduce the weight of the panels [6]. Therefore, lightweight concrete structures are increasingly used, e.g., channel slabs or bubble deck slabs. This approach aims to eliminate the concrete that does not fulfill any structural functions to reduce the weight and thus, the dead load [7,8].

Over the last few decades, many numerical models have been developed to represent the global behavior of prefabricated concrete structures and to understand their mechanical behavior. These models serve as valuable tools for simulating and analyzing the structural response of prefabricated elements, enabling engineers to evaluate their performance under various loading conditions and optimize their design. For instance, the paper [9] presented a full 3D model of prefabricated bridge slabs for the purpose of modelling their non-linear behavior using the constitutive model of concrete damage plasticity. In turn, the bending behavior of composite slabs was analyzed by Tzaros et al. [10]. Gholamhossein et al. [11] proposed a three-dimensional solid finite element model to investigate the connection between concrete and steel. Information regarding the puncture resistance of concrete slabs can be found in paper [12]. Using finite element method (FEM), it becomes possible to analyze structures with complex shapes and geometries, and to gain insight into the non-linear behavior of concrete and steel [13-15]. However, that detailed modeling of three-dimensional prefabricated slabs requires a lot of work, specialist knowledge, as well as, the use of specific software and is very time-consuming in terms of calculations. The solution to the problem may be the use of one of the homogenization methods.

Homogenization is a mathematical technique used to analyze and model the behavior of heterogeneous materials or structures. It aims to capture the effective properties of an entire material or structure, taking into account its constituent materials or components. In the context of construction and structural calculations, homogenization refers to the simplification or adoption of uniform material or structure properties in order to facilitate calculations. For materials with an irregular structure or composition, simplifications can be used where the material is treated as having uniform properties such as strength, stiffness and density. Homogenization can also refer to simplification in structural analysis, where complex models of structural elements or details are replaced by simpler models that take into account similar structural behavior. One can distinguish, among others, the method of periodic homogenization [16], non-linear homogenization [17] or the method of multi-scale homogenization based on genome mechanics [18]. A slightly different approach can be found in the work of Garbowski and Marek [19], where a method based on reverse analysis was used. On the other hand, in the work [20], a method of homogenization based on strain energy for sandwich panels with a honeycomb core was presented. Biancolini, on the other hand, developed a method of strain energy equivalence between the simplified model and the representative volumetric element (RVE) model [21]. This method was then extended in [22]. Homogenization may introduce some simplifications and approximations, so its use should be carefully assessed in the

 doi:10.20944/preprints202306.1270.v1

context of a specific project and the fulfillment of relevant load-bearing and safety requirements.

Homogenization methods are also used in structural optimization analyses. It refers to the process of designing and modifying a building or structural elements to achieve the best possible results in terms of strength, cost-effectiveness and energy efficiency. In addition, structural optimization is a complex process that requires consideration of multiple parameters and various engineering disciplines. It includes the integration of knowledge from structural engineering, materials science, mechanical engineering, and other relevant fields. The goal of the optimization is to find the best compromise between individual design requirements, so that the construction is as efficient, durable and economical as possible, taking into account factors such as structural loads, material properties, construction techniques and environmental impacts. This process may include the analysis of various scenarios, e.g., changing the geometry, materials, configuration of structural elements to find the most suitable solution. The use of advanced tools such as structural analysis software and computer simulations can greatly facilitate the optimization process and help in obtaining optimal design solutions. These tools allow engineers to model and simulate the behavior of the structure under various conditions, accurately predict its performance and evaluate different design alternatives.

Many studies have been conducted that provide information on the optimization of building construction, e.g., prefabricated elements, steel or wooden structures. Sotiropoulos et al. presented a conceptual design method based on topology optimization using prefabricated structural elements [23]. The hybrid optimization method was used to optimize cellular beams in [24]. The optimization of thin-walled cross-sections was shown in [25]. Furthermore, the work by Sojobi et al. [26] presented a multi-objective optimization of a prefabricated Carbon fiber reinforced polymer (CFRP) composite sandwich structure. Additionally, Xiao and Bhola [27] presented the design of prefabricated building systems using building information modelling (BIM) technology and structural optimization. In the work by Xie et al. [28], a genetic algorithm was utilized for optimal planning of prefabricated construction projects.

The paper presents an algorithm for the optimal design of bubble deck construction in order to minimize the amount of concrete and ensure that the permissible deflection arrow of the structure in the serviceability limit state are not exceeded. To simplify the model and speed up the analysis, the numerical homogenization method based on the equivalence of the strain energy between the simplified shell model and the three dimensional reference RVE bubble deck model was used. The analyzed concrete slab contains evenly distributed voids over the entire surface and both upper and lower steel reinforcement, which increases the complexity and time of the calculations. Therefore, the original numerical homogenization method, initially developed for shell structures, was modified. In the work, an extension of the method was used to simultaneously include continuum and truss elements, similarly to [29,30].

2. Materials and Methods

2.1. Lightweight concrete slabs

2.1.1 Voided floor slabs

The expression “voided floor slabs” refers to a special type of construction where the concrete slab contains a system of regular hollows or empty spaces inside. The hollows may have various shapes such as spheres, cylinders, clovers, etc. In addition, they can be arranged in a specific pattern or grid. Voided floor slabs are used to achieve greater efficiency in terms of material use and to reduce the weight on the structure while ensuring the required strength and performance of the floor structure. One of the most common types of voided floor slabs is the bubble type ceiling.

 doi:10.20944/preprints202306.1270.v1

The bubble deck is a modern ceiling solution compared to traditional slabs, in which the ineffective concrete in the middle of the cross-section is replaced by voids. This floor slab was invented in the nineties of the last century by Danish engineer Jorgen Breuning [31]. It is used in residential, office, industrial and utility buildings. In addition, the bubble deck ceiling is used in factories, parking structures, schools and hotels.

Bubble deck has spherical or elliptical voids [32] evenly distributed over the entire surface, without changing the two-way action of the element. This solution allows to reduce the amount of concrete by 33% and price by 30% compared to traditional solid slabs with the same parameters [33]. One of the main differences between solid slabs and bubble deck is their shear resistance [34]. In addition, by adjusting the appropriate reinforcement mesh and hole geometry, an optimized concrete structure can be achieved, allowing for the simultaneous maximum utilization of both moment and shear zones.

The height of such slabs can achieve up to 600 mm, which allows for a span of up to 20 m. On the other hand, the diameter of the bubble made of HDPE (high-density polyethylene) varies between 180 and 450 mm, depending on the designed thickness of the slab. The HDPE material used come from recycled plastic waste. Therefore, the above solution contributes to the reduction of pollution and has a positive impact on environmental protection. However, the distance between the individual voids in the bubble deck system must be at least 1/9 of the bubble diameter. This requirement ensures adequate structural integrity and optimal load distribution in the floor slab. By keeping the distance between voids to a minimum, the system can effectively reduce the weight of the structure while providing sufficient strength and stability. The voids are fixed in special steel baskets between the upper and lower reinforcement of the plate to prevent their displacement during concrete pouring [35,36]. In addition, the slab is connected directly to concrete columns or walls in situ without any beams, providing a wide range of structural cost and benefits. This eliminates the need for additional structural elements, simplifies the construction process, and allows for more flexible design options. Such a direct connection between the slab and columns or walls enhances structural efficiency and optimizes construction costs.

There are 3 methods of manufacturing bubble deck: (i) in-situ approach – Figure 1a, (ii) semi-prefabricated elements (Filigree element) – Figure 1b and (iii) prefabricated panels – Figure 1c [37]. In the case of the in-situ approach (i), the slabs are made directly on site at the place of their installation. Voids are placed in specific places between the bottom and top reinforcement of the floor. In the next step, the finished modules are placed on the prepared formwork. Then the slab is concreted. It is worth noting that this solution is very effective in buildings where the floor is not flat, e.g. there is a domed or curved ceiling. In the case of approach (ii), the deck is semi-prefabricated bubble deck. This means that elements are created in the production plant, which then require additional concreting at the construction site. This is a combination of methods (i) and (iii). The lower part of the ceiling, which is also the permanent formwork, is in the form of a concrete slab with a thickness of approximately 6 cm. In addition, it has both lower and upper reinforcement with spaced voids. Then, the whole element is transported to the construction site and concreted after moving to the appropriate place. In contrast, approach (iii) deals with components that are fully manufactured. The finished prefabricated elements are transported to the construction site. This solution partially limits the ability of the plates to function as bi-directional. The solution to this problem may be the proper design of the connection between the prefabricated slabs, which will enable the use of prefabricated elements as two-way floors, similarly to approaches (i) and (ii).

(a)

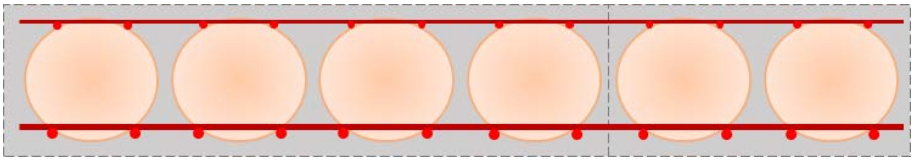

 doi:10.20944/preprints202306.1270.v1

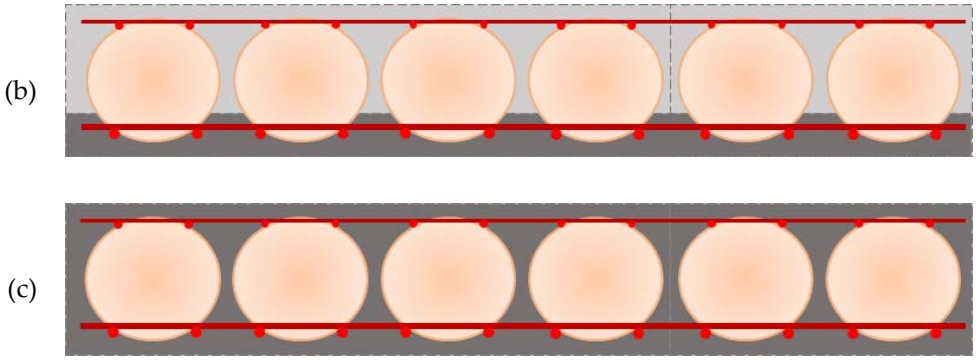

Figure 1. Types of bubble deck: (a) in-situ element, (b) semi-prefabricated element, (c) fully prefabricated element.

Bubble deck is generally designed using conventional solid ceiling design methods in accordance with applicable international and local design standards. The above floor system is a true bidirectional monolithic slab and behaves like a solid slab in both elastic and plastic modes. This means it can effectively carry and distribute loads in a manner similar to traditional solid slabs, ensuring structural integrity and performance. Besides, it mainly uses two analysis methods in design, such as Linear Elastic and Yield Line method. Thanks to the optimized geometry and spherical bubbles, every part of the concrete in the slab is actively involved and relevant in the calculation of different types of forces.

2.1.2. Serviceability limit state of bubble deck concrete slabs

During the design and analysis structures, it is important to check two main limit states to ensure the safety and strength of the structure. It is the ULS – ultimate limit state and SLS – serviceability limit state. The first one concerns the assessment of the load capacity of the structure and checking whether it is able to withstand loads, in accordance with the adopted standards, building regulations and design requirements. For different types of structures, such as floors, columns, foundations, bridges, etc., ULS refers to the evaluation of their strength in response to various forces, such as compression, bending, tension, bending moments, shear forces, etc. The strength of bubble deck is typically determined by structural analysis and calculation, taking into account factors such as flexural strength, shear capacity and the ability to distribute loads efficiently.

The serviceability limit state (SLS) refers to the conditions in which the structure can be operated without unacceptable deformations or damage that may affect its functionality and safety. In the case of bubble boards, the key aspect is to ensure that the bubbles inside the board are stable and do not undergo deformation or damage that could affect the load capacity and stiffness of the board. SLS covers various aspects including deflections and cracks. In the case of slabs, there are certain permissible deflection limits that should not be exceeded to ensure the stability and functionality of the structure. Excessive deflections can lead to improper functioning of finishing elements, problems with water drainage or deterioration of interior aesthetics. Usually, when assessing the SLS, it is recommended to examine the cracks to determine their nature, size and impact on the safety and functionality of the structure.

In this work, analyzes of the optimization of the bubble deck ceiling in terms of SLS were carried out. It was assumed that the maximum plate deflection cannot exceed the permissible value equal to 1/250 of the span between supports according to [38] for the quasi-permanent load case. In addition, it was assumed that the floor is located in an office building and is subjected to the following loads evenly distributed over the entire surface of the slab. One of them is the useful load with a characteristic value of $q_k = 3\ \mathrm{kN/m^2}$ (according to [39] for office rooms). In addition, it was assumed that an equivalent load from partition walls equals to $q_k = 0.8\ \mathrm{kN/m^2}$ and a permanent load outside the weight

Preprints (www.preprints.org) | NOT PEER-REVIEWED | Posted: 19 June 2023 doi:10.20944/preprints202306.1270.v1

of the slab structure with a value of $g_k = 1.5\ \mathrm{kN/m^2}$ are applied to the ceiling. The ceiling weight is a variable value and depends on the geometrical parameters of the slab and bubble cross-section, so it was taken into account directly in the cost function of the optimization algorithm. The deflection arrow was determined for the case of quasi-permanent loads at the serviceability limit state, therefore the factors reducing the load values according to [39] were applied.

2.2. Numerical homogenization of slab

In the following work, the method of numerical homogenization based on the equivalence of strain energy between the three-dimensional reference model and the simplified shell model was used [19,29,30,40-43]. The above method has already been adapted to prefabricated concrete slabs reinforced with spatial trusses [30] and reinforced slabs with voids such as bubble deck [29]. This approach uses the classical formulation of the displacement-based finite element method. Extracting individual values for internal nodes - subscript "i" and external nodes - subscript "e":

$$\mathbf{K}\,\mathbf{u} = \mathbf{F} \;\rightarrow\; \begin{bmatrix} \mathbf{K}_{ee} & \mathbf{K}_{ei} \\ \mathbf{K}_{ie} & \mathbf{K}_{ii} \end{bmatrix} \begin{bmatrix} \mathbf{u}_e \\ \mathbf{u}_i \end{bmatrix} = \begin{bmatrix} \mathbf{F}_e \\ \mathbf{0} \end{bmatrix}. \tag{1}$$

where: $\mathbf{K}$ is the stiffness matrix, $\mathbf{u}$ is a displacement vector of nodes and $\mathbf{F}$ is the external nodal load vector.

For this purpose, it is necessary to separate a representative volume element (RVE) from the model and perform static condensation. Condensation is the elimination of secondary degrees of freedom, in this case, internal nodes. Then, it is necessary to redefine the stiffness matrix with a reduced number of degrees of freedom only at the external nodes, see Figure 2a.

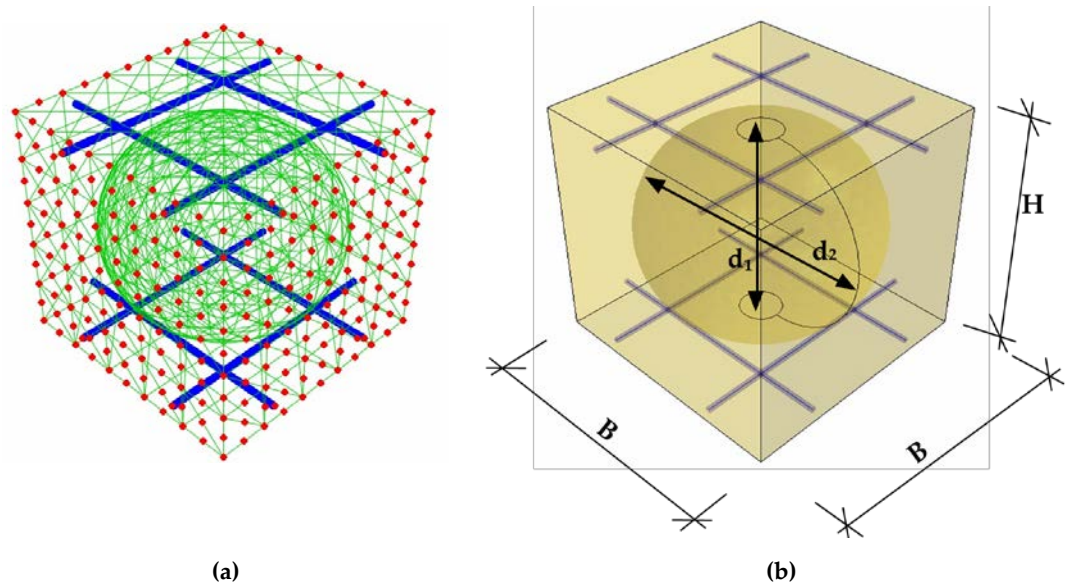

Figure 2. RVE: (a) external (in red color) and internal nodes and (b) parametrized for optimization purpose.

Additionally, the presented method of homogenization uses the relationship between the total energy of elastic deformation stored in the system after static condensation and the work of external forces on appropriate displacements

$$E = \frac{1}{2}\mathbf{u}_e^T\,\mathbf{F}_e \tag{2}$$

Preprints (www.preprints.org) | NOT PEER-REVIEWED | Posted: 19 June 2023 doi:10.20944/preprints202306.1270.v1

The homogenization method, as in [29,30], has been modified here to include only translational degrees of freedom (for two types of finite elements used in the models - truss and continuum). Therefore, the relationship between the generalized strain constants and the location of the external RVE nodes is expressed by the following transformation.

$$\begin{bmatrix} u_x \\ u_y \\ u_z \end{bmatrix}_i = \begin{bmatrix} x & 0 & y/2 & z/2 & 0 & xz & 0 & yz/2 \\ 0 & y & x/2 & 0 & z/2 & 0 & yz & xz/2 \\ 0 & 0 & 0 & x/2 & y/2 & -x^2/2 & -y^2/2 & -xy/2 \end{bmatrix}_i \begin{bmatrix} \varepsilon_x \\ \varepsilon_y \\ \gamma_{xy} \\ \gamma_{xz} \\ \gamma_{yz} \\ \kappa_x \\ \kappa_y \\ \kappa_{xy} \end{bmatrix}_i, \tag{3}$$

Then, after appropriate transformations, we can obtain the stiffness matrix $\boldsymbol{A}_k$, which is the ABDR matrix, consisting of all the required compression, bending and shear stiffnesses.

$$\mathbf{A}_k = \begin{bmatrix} \mathbf{A}_{3\times 3} & \mathbf{B}_{3\times 3} & 0 \\ \mathbf{B}_{3\times 3} & \mathbf{D}_{3\times 3} & 0 \\ 0 & 0 & \mathbf{R}_{2\times 2} \end{bmatrix} \tag{4}$$

More information on numerical homogenization based on strain energy equivalence can be found in the works [19,29,30,40-43].

The design parameters, $\bar{x}$, that were used to determine the representative RVE for a specific design of the bubble bridge slab in the analyzed optimization problem are shown in Figure 2b. The assumed designed parameters reads:

$$\bar{x} = \{B, H, d_1, d_2\} \tag{5}$$

in which B is the width and length of RVE concrete unit, H the height of the RVE concrete unit and d_1, d_2 are the dimensions of the ellipsoidal void, height and horizontal diameter, respectively.

2.3. Study framework and optimization problem definition

In everyday challenges, structural engineers tackle various problems, one of the most common one is the optimal design of the structure. In this paper, the optimal design of bubble deck slab in regards to not exceeding the serviceability limit state (SLS) and minimal use of the concrete is analyzed. The problem is not trivial since the bubble deck slabs have variable cross-section, in regions with full concrete cross-section the plate has bigger stiffness, while for bubble void regions the plate is less stiff. The properties of the plate are varying periodically across the span, which makes difficult to calculate the displacement field of such slab. Also, the minimal use of the concrete is opposed to limiting plate deflection. Therefore, the typical approach for computations must be extended in order to meet the requirements of SLS and limit the material use.

In this paper, the numerical homogenization technique was used to determine the effective bending stiffness for the usage of computing the plate displacement via analytical formula. The homogenization technique used was the one presented by Garbowski and Gajewski [22]. The bending stiffnesses of D_{11}, D_{22}, D_{12} and D_{33} were determined by the homogenization technique [22], which was used in multiple papers [29, 40, 41, 42, 43].

The square and symmetric bubble deck concrete slab was considered here, the structure was reinforced with upper and lower steel mesh with $\phi 10$ steel bars. The cross-section design of the concrete bubble deck was described by a parametric RVE model with design parameters gathered in $\bar{x}$, see Section 2.2. The span dimensions of the slab are assumed to be $12 \times 12\ m^2$ with evenly distributed load q_0, see Section 2.1.2 for more details of the load assumed.

The governing equation for Kirchhoff-Love plate takes the following form [44,45]:

Preprints (www.preprints.org) | NOT PEER-REVIEWED | Posted: 19 June 2023 doi:10.20944/preprints202306.1270.v1

$$D_{11}\frac{\partial^4 w}{\partial x^4} + 2(D_{12} + 2D_{33})\frac{\partial^4 w}{\partial x^2 \partial y^2} + D_{22}\frac{\partial^4 w}{\partial y^4} = q. \quad (6)$$

in which w is the transverse deflection, x and y are the in-plane coordinates of the plate and q is the transverse load.

The plate assumed is simply supported for all edges, therefore:

$$\begin{aligned} a: x_1 = 0, \quad w = 0, \quad M_1 = 0. \\ b: x_2 = 0, \quad w = 0, \quad M_2 = 0. \end{aligned} \quad (7)$$

in which a, b are the dimensions of the floor slab (here $a = 12\,m$ and $b = 12\,m$ were assumed) and x_1, x_2 are the orthogonal coordinates along the perpendicular edges, respectively.

It was assumed that the orthotropic plate is subjected to transverse uniformly distributed load, labelled as q_0:

$$q(x_1, x_2) = q_0 = q_0(\bar{x}). \quad (8)$$

For more details regarding determining uniformly distributed load, q_0, please refer to Subsection 2.1.2.

The final form of the plate deflection reads:

$$w(\bar{x}) = \frac{16 q_0}{\pi^6} \sum_{m=1}^{\infty}\sum_{n=1}^{\infty} \frac{\sin\frac{m\pi x_1}{a}\sin\frac{n\pi x_2}{b}}{mn\left[D_{11}(\bar{x})\left(\frac{m}{a}\right)^4 + 2\left(D_{12}(\bar{x}) + 2D_{33}(\bar{x})\right)\left(\frac{mn}{ab}\right)^2 + D_{22}(\bar{x})\left(\frac{n}{b}\right)^4\right]}. \quad (9)$$

in which m, n are the odd numbers.

The total cost function, F, in the optimization problem to be solved takes two following components:

$$F(\bar{x}) = \omega F_{vol}(\bar{x}) + F_{defl}(\bar{x}). \quad (10)$$

in which F_{vol} is responsible for decreasing the concrete use and F_{defl} regards not exceeding the serviceability limit state due to Eurocode standard [38]. Dimensionless factor ω is the scaling factor of the previous two and was selected by trial and error with the aim of balancing the influence of both components on the objective function. Therefore, in the study, ω was set to $0.2e-9$. The mathematical details of the optimization algorithm used for minimizing the cost function $F(\bar{x})$ were included in Section 2.4.

The total volume of a bubble deck floor slabs, F_{vol}, was calculated by using a single representative volume element of the bubble deck unit:

$$V_{RVE}(\bar{x}) = B \cdot L \cdot H - \frac{4}{3}\pi\frac{d_1}{2}\left(\frac{d_2}{2}\right)^2. \quad (11)$$

Therefore, in the first component of the cost function, F_{vol} reads:

$$F_{vol}(\bar{x}) = \frac{ab}{BL} V_{RVE}(\bar{x}). \quad (12)$$

Second component of the cost function, F_{defl}, is computed based on the maximal slab deflection (computed by Equation (9)) combined with the serviceability limit state:

$$F_{defl}(\bar{x}) = \left| w(\bar{x}) - \frac{\min(a,b)}{250} \right|. \quad (13)$$

In the optimization problem, the boundary limits of each design parameter of the concrete bubble deck were assumed and were presented in Table 1. b_{min} is the lower,

Preprints (www.preprints.org) | NOT PEER-REVIEWED | Posted: 19 June 2023 doi:10.20944/preprints202306.1270.v1

while b_{max} is the upper boundary of the physical dimensions. In Section 2.2, full details regarding the meaning of the symbols is presented, including exemplary graphics.

Due to the fact that the dimensions of the bubble change in the optimization process and that the bubble is immersed in concrete with a variable height and width of the RVE module, physical inequality restrictions should be introduced. Therefore, the following inequality constraints were adopted:

$$\begin{aligned} d_1 - H + 40 \leq 0 \\ d_2 - B + 40 \leq 0 \end{aligned} \tag{14}$$

In Equations (14), 40 represents the concrete bubble cover in mm, that is, the distance between the surface of bubble void and the outer surface of the concrete at cardinal points. The assumed nominal value of the concrete cover in regard to steel mesh was $35\ mm$.

Table 1. The lower and upper boundary values of the parameters selected for optimization of the concrete part of the bubble deck slab.

boundary	B (mm)	H (mm)	d_1 (mm)	d_2 (mm)
b_{min}	100	100	50	50
b_{max}	500	500	500	500

Local search algorithms, such the one used in the paper, are vulnerable to find the locally optimal solutions. Therefore, in order to minimize the probability that a globally and not locally optimal solution will be found, the optimization algorithm was ran many times from different starting points (initial guesses), see Table 2. This is a typical approach for better exploration of the multi-dimensional space of design parameters.

All computations in the research, apart computing stiffness matrices of RVEs (see Section 2.2), were performed in MATLAB software [46].

Table 2. The initial guesses of design parameters selected for optimization of the concrete part of the bubble deck slab.

No.	B (mm)	H (mm)	d_1 (mm)	d_2 (mm)
$\bar{x}^0{}_1$	150	300	100	70
$\bar{x}^0{}_2$	250	200	150	80
$\bar{x}^0{}_3$	220	200	160	100
$\bar{x}^0{}_4$	200	250	110	180
$\bar{x}^0{}_5$	170	150	90	90

2.4. Mathematical optimization procedure

Among many available methods of optimization, the sequential quadratic programming (SQP) method is one of the most reliable and trustworthy. This mainly regards to its efficiency, namely, the smallest number of cost function evaluations is obtained in the benchmark examples and sufficient accuracy is maintained [47-51]. Therefore, in this study, SQP method was used, likewise in [52].

The classical optimization problem reads [51]:

$$\min F(\bar{x}), \tag{15}$$

in which $F(\bar{x})$ is the cost function of sought parameters $\bar{x}$. The sough parameters may be constrained with equalities:

$$\begin{aligned} C_{eq}(\bar{x}) = 0, \\ A_{eq} \cdot \bar{x} = b_{eq}, \end{aligned} \tag{16}$$

Preprints (www.preprints.org) | NOT PEER-REVIEWED | Posted: 19 June 2023 doi:10.20944/preprints202306.1270.v1

or/and more complex constraints may be more adequate. For instance, nonequality constraints:

$$\begin{gathered} C(\bar{x}) \leq 0, \\ A \cdot \bar{x} \leq b, \\ b_{min} \leq \bar{x} \leq b_{max}, \end{gathered} \tag{17}$$

in which b, b_{eq} are one-column matrices; A, A_{eq} are matrices; C and C_{eq} are functions. b_{min} and b_{max} represents lower and upper boundaries of sought parameters $\bar{x}$.

Constraints in function $F(\bar{x})$ are computed by utilizing the Lagrange's function approach, L. Thus, mathematically equivalent subproblem is defined by the following:

$$L(\bar{x}, \lambda) = F(\bar{x}) + \sum_{i=1}^{m} \lambda_i \cdot g(\bar{x}), \tag{18}$$

in which λ_i are the so-called Lagrange multipliers, while $g_i(\bar{x})$ are the constraints of nonequality.

In SQP method, the following form of quadratic programming is solved:

$$\min_{d \in R^n} \frac{1}{2} d^T H_k + \nabla F(\bar{x}_k)^T d, \tag{19}$$

in which H_k is the positive definite approximation of Hessian, which approximates the Equation (18). The approximation of Hessian matrix is modified at each primary iteration by Broyden–Fletcher–Goldfarb–Shanno (BFGS) method:

$$H_{k+1} = H_k + \frac{q_k q_k^T}{q_k^T s_k} - \frac{H_k s_k s_k^T H_k^T}{s_k^T H_k s_k}, \tag{20}$$

in which

$$s_k = \bar{x}_{k+1} - \bar{x}_k, \tag{21}$$

$$q_k = \left(\nabla F(\bar{x}_{k+1}) + \sum_{i=1}^{m} \lambda_i \nabla g_i(\bar{x}_{k+1}) \right) - \left(\nabla F(\bar{x}_k) + \sum_{i=1}^{m} \lambda_i \nabla g_i(\bar{x}_k) \right). \tag{22}$$

New step is computed basing on the solution of the quadratic programming problem:

$$\bar{x}_{k+1} = \bar{x}_k + \alpha_k d_k, \tag{23}$$

in which α_k is the step length obtained by minimization of the objective function. [47-51].

3. Results

In local search optimization algorithms, it is recommended to solve multiple optimization problems to determine the solution, which is, not locally, but globally optimal. Therefore, the optimization procedure was conducted for several initial guesses of design parameters to find the best solution, the solutions of initial guesses assumed were presented in Section 2.3. The results obtained from solving the optimization problem stated in Sections 2.3 by the optimization method shown in Section 2.4 were summarized in Table 3. The second to five columns present the optimal parameters of the concrete bubble deck designs. In column six, the slab deflection obtained for optimal designs due to the uniformly distributed load may be found. Moreover, the seventh to ninth columns show the components of the cost function and the total value of the cost function.

Table 3. Optimal designs of concrete bubble deck slab with corresponding cost function values obtained by optimization algorithm.

No.	B (mm)	H (mm)	d_1 (mm)	d_2 (mm)	w (mm)	ωF_{vol} (–)	F_{defl} (–)	F (–)
$\bar{x}^0{}_1$	100.0	158.6	115.8	50.0	47.94	4.1314	0.0616	4.1930

Preprints (www.preprints.org) | NOT PEER-REVIEWED | Posted: 19 June 2023 doi:10.20944/preprints202306.1270.v1

$\bar{x}^0{}_2$	122.1	158.5	109.1	55.9	48.02	4.2193	0.0164	4.2357
$\bar{x}^0{}_3$	158.2	157.5	99.7	89.1	48.01	4.0593	0.0121	4.0714
$\bar{x}^0{}_4$	110.7	156.0	52.8	70.5	48.12	4.2505	0.1165	4.3669
$\bar{x}^0{}_5$	144.8	155.6	53.8	104.4	48.04	4.0600	0.0390	4.0990

More details of the convergence of the solutions are presented for selected exampled from Table 3 in Figures 3–5. In each figure, the minimization of the cost function, F, was demonstrated with its components for iterations of the optimization algorithm, i.e., ωF_{vol} – component of minimizing the volume of the concrete and F_{defl} – component of minimizing the maximum plate deflection, see Figures 3a–5a. Also, in Figures 3b–5b, the maximum plate deflection was confronted with the SLS condition from Eurocode standard [38]. For the analyzed case of the slab, namely, $12 \times 12\ m^2$, the limit computed from $1/250$ condition equals $48\ mm$. In Figures 3b–5b, the limit was marked with dashed line. Also, in Figures 3c–5c, the changes of the sought parameters of B, H, d_1 and d_2 within optimization were shown, what shows the convergence to the final sought parameters of the bubble deck slab.

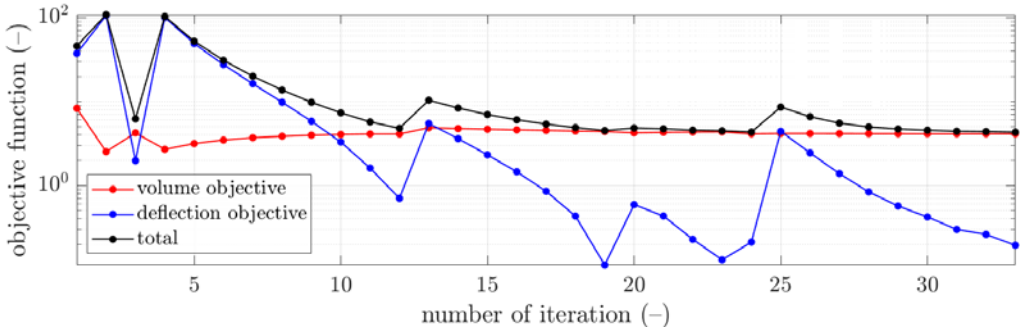

(a)

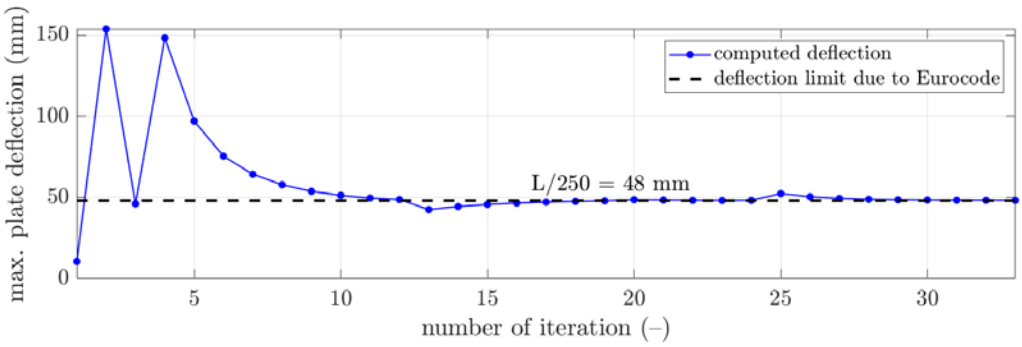

(b)

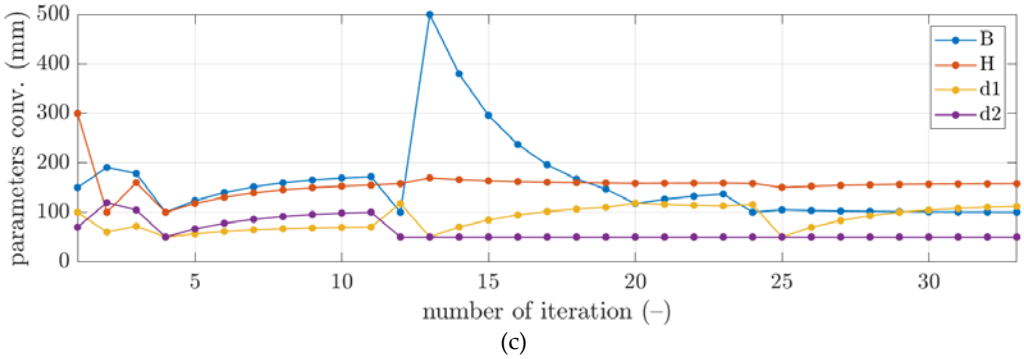

(c)

Preprints (www.preprints.org) | NOT PEER-REVIEWED | Posted: 19 June 2023 doi:10.20944/preprints202306.1270.v1

Figure 3. The convergence of the process of optimal selection of geometrical parameters of the bubble deck slab based on the criterion of concrete use and the fulfillment of the serviceability limit state for initial guess $\bar{x}^0{}_1$: (a) cost function, (b) verification of serviceability limit state and (c) bubble deck parameters derived.

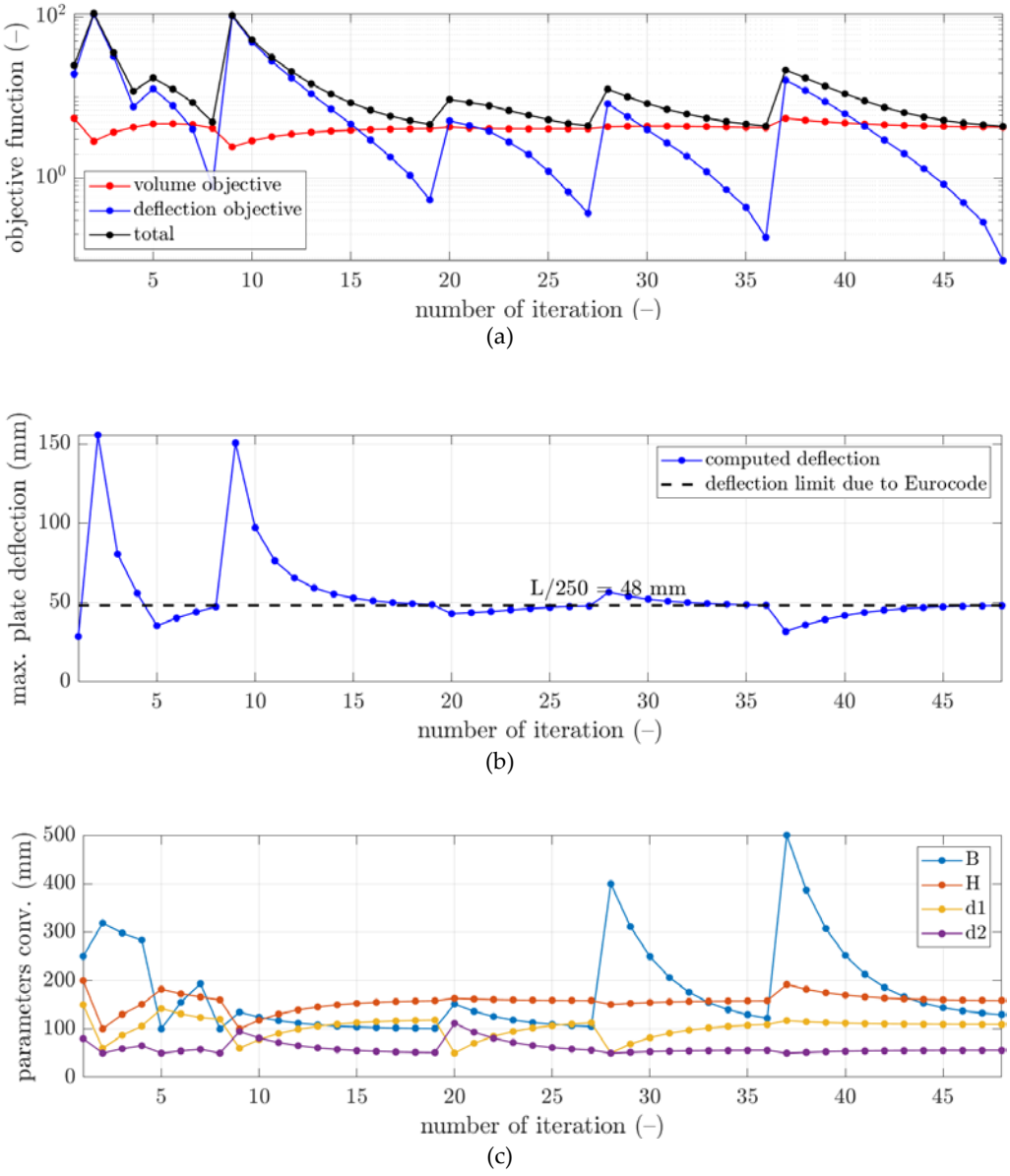

Figure 4. The convergence of the process of optimal selection of geometrical parameters of the bubble deck slab based on the criterion of concrete use and the fulfillment of the serviceability limit state for initial guess $\bar{x}^0{}_2$: (a) cost function, (b) verification of serviceability limit state and (c) bubble deck parameters derived.

Preprints (www.preprints.org) | NOT PEER-REVIEWED | Posted: 19 June 2023 doi:10.20944/preprints202306.1270.v1

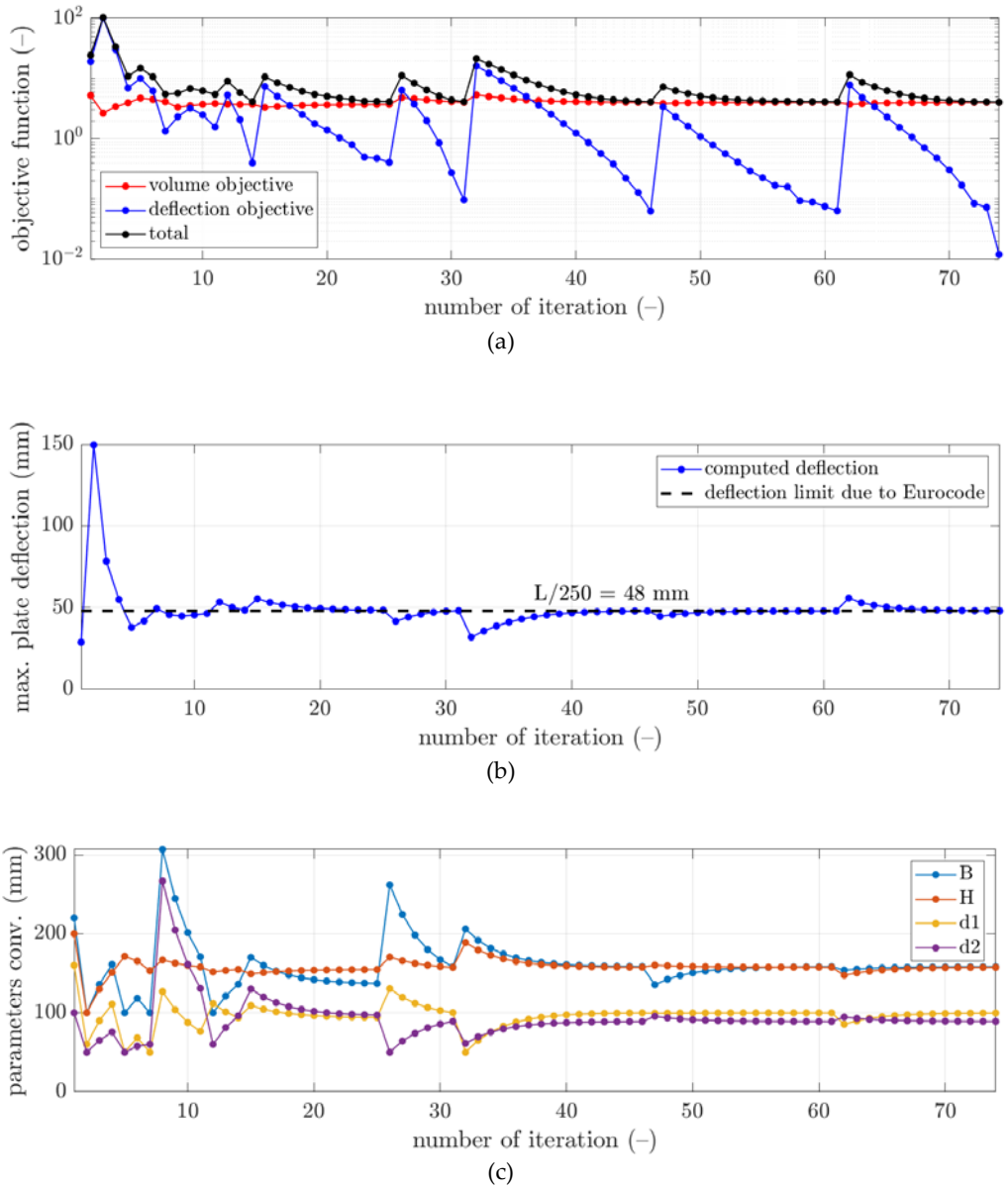

Figure 5. The convergence of the process of optimal selection of geometrical parameters of the bubble deck slab based on the criterion of concrete use and the fulfillment of the serviceability limit state for initial guess $\bar{x}^0{}_3$: (a) cost function, (b) verification of serviceability limit state and (c) bubble deck parameters derived.

4. Discussion

Optimal design of bubble deck slab floor in regard to concrete use and SLS is not trivial task. The main difficulty is determining the mechanical properties of periodically changing cross-section of the plate. Full detailed finite element modelling of such structures is time-consuming in modelling and computations. Therefore, for this reason, for engineering purpose, the method presented in the paper is highly attractive. It does not require full formal finite element analysis of the floor slab, but only building the global stiffness matrix of the single periodic RVE unit and straightforward post computations to receive effective stiffnesses.

Therefore, in the paper, the complex structure of bubble deck slab was considered to determine the optimal solution without using a typical, less accurate methods. In the paper, the minimization of F_{vol} and F_{defl} components are in contrary, therefore, it is typical

that the F_{vol} component decreases, while F_{defl} component increases, for instance see iterations 2 and 9 in Figure 4a.

However, as presented in the optimization summary in Section 3, it was possible to obtain the deflection very close to the design standard limit, i.e., $48\,mm$. As shown in Table 3, all differences in the deflections achieved in relation to the design standard limit, were approximately not bigger than $0.15\,mm$. Therefore, those components in the cost function outcomes were relatively small, not bigger than 0.12, however, the smallest was computed for the initial guess of $\bar{x}^0{}_3$., i.e., 0.0121. In Figures 3b–5b, it may be observed that every once in a while the optimization algorithm breaks the deflection limitation, for instance see iterations 2 and 4 in Figure 3b, but it returns to respect the limit after one or few iterations. Similar features are visible in Figure 4b – iterations 2 and 9, and in Figure 5b – iterations 2, 12 and 15.

On the other hand, it may be observed that the component related with the minimization of the concrete use gives much greater values, that is, between 4.06 and 4.25. Since this component is the scaled volume of the concrete of the slab it cannot be minimized to 0. Still, the significant decreases of this component can be observed compared to the initial guess values, see red plots in Figures 3a–5a. Here, the lowest value was obtained for the initial guess of $\bar{x}^0{}_3$., i.e., 4.0593.

The best solution, that is, globally optimal solution was obtained for the initial guess of $\bar{x}^0{}_3$. Therefore, the optimal parameters of bubble deck slab of $12 \times 12\,m^2$ for uniformly distributed load are: $B = 158.2\,mm$, $H = 157.5\,mm$ $d_1 = 99.7$ mm and $d_2 = 89.1\,mm$. Optimal parameter H was similar for all locally optimal solutions, as it may be observed in Table 3, it changes from 155.6mm to 158.6 mm.

The main advantage of the methodology shown in the paper is the computational time of the analysis. The single evaluation of the cost function lasts less than 15 seconds. Therefore, approximately in less than 20 minutes the single optimization procedure was finished. Going further, after about 2 hours the reasonable exploration of the design space can be achieved and final, globally optimal solution may be expected.

5. Conclusions

The main aim of the paper was to find the optimal designs of the bubble deck slab subjected to uniformly distributed load in regard to minimal concrete use and not exceeding the serviceability limit state of the Eurocode standard. In the research study, the numerical homogenization technique was used to determine the effective properties of the bubble deck slab within the cost function. Moreover, the local search algorithm of sequential quadratic programming was used in the minimization problem with linear constraints to derive bubble deck slab module, that is, its length/width and height, but also the geometry of the ellipsoidal bubble void, i.e., its height and horizontal diameter.

As confirmed in the study, the optimization study allowed to determine designs of the bubble deck slabs that ensure the minimum mass of concrete and meet the serviceability limit state. It was shown that the homogenization method used in the paper is highly attractive because it does not require solving complex structural problem through computationally expensive finite element method. In the paper, the complex structure of bubble deck slab was considered without using a typical, less accurate, method of substitute cross-section of the concrete.

Author Contributions: conceptualization, T.G. (Tomasz Garbowski); methodology, T.G. (Tomasz Gajewski) and T.G. (Tomasz Garbowski); software, T.G. (Tomasz Gajewski) and N.S.; validation, T.G. (Tomasz Garbowski), T.G. (Tomasz Gajewski) and N.S.; formal analysis, T.G. (Tomasz Gajewski) and N.S.; investigation, N.S. and T.G. (Tomasz Gajewski); writing—original draft preparation, T.G. (Tomasz Gajewski) and N.S.; writing—review and editing, T.G. (Tomasz Gajewski), T.G. (Tomasz Garbowski) and N.S.; visualization, T.G. (Tomasz Gajewski) and N.S.; supervision, T.G. (Tomasz Garbowski) and T.G. (Tomasz Gajewski); funding acquisition, T.G. (Tomasz Garbowski). All authors have read and agreed to the published version of the manuscript

Funding: This research received no external funding.

Institutional Review Board Statement: Not applicable.

Informed Consent Statement: Not applicable.

Data Availability Statement: The data presented in this study are available on request from the corresponding author.

Acknowledgments: The authors also acknowledge the grant of the Ministry of Education and Science, Poland, from Poznan University of Technology for Young Researchers; grant number 0411/SBAD/0009.

Conflicts of Interest: The authors declare no conflict of interest. The funders had no role in the design of the study; in the collection, analyses, or interpretation of data; in the writing of the manuscript, or in the decision to publish the results.

References

1. Feng, D.; Wu, G.; Lu, Y. Finite element modelling approach for precast reinforced concrete beam-to-column connections under cyclic loading. *Eng. Struct.* **2018**, *174*, 49–66.
2. Baran, E. Effects of cast-in-place concrete topping on flexural response of precast concrete hollow-core slabs. *Eng. Struct.* **2015**, *98*, 109–117.
3. Ramírez-Torres, A.; Di Stefano, S.; Grillo, A.; Rodríguez-Ramos, R.; Merodio, J.; Penta, R. An asymptotic homogenization approach to the microstructural evolution of heterogeneous media. *Int. J. Non-Linear Mech.* **2018**, *106*, 245–257, doi:10.1016/j.ijnonlinmec.2018.06.012.
4. Szymczak-Graczyk, A.; Ksit, B.; Laks, I. Operational Problems in Structural Nodes of Reinforced Concrete Constructions. *IOP Conference Series: Materials Science and Engineering* **2019**, 603(3), 032096. https://doi.org/10.1088/1757-899X/603/3/032096
5. Lichołai L Budownictwo ogólne. Tom 3. Elementy budynków podstawy projektowania, Arkady, Warszawa, 2008 (in polish)
6. Ksit, B.; Szymczak-Graczyk, A. Rare weather phenomena and the work of large-format roof coverings. *Civil and Environmental Engineering Reports* **2019**, 29 (3), 123-133. https://doi.org/10.2478/ceer-2019-0029
7. Mirajkar, S.; Balapure, M.; Kshirsagar, T. Study of Bubble Deck Slab. *International Journal of Research in Science & Engineering* **2017**, 7, 1-5.
8. Quraisyah, A.D.S.; Kartini, K.; Hamidah, M.S.; Daiana K. Bubble Deck Slab as an Innovative Biaxial Hollow Slab – A Review. *Journal of Physics: Conference Series* **2020**, 1711(1), 012003. https://doi.org/10.1088/1742-6596/1711/1/01/2003
9. Ren, W.; Sneed, L.H.; Yang, Y.; He, R. Numerical Simulation of Prestressed Precast Concrete Bridge Deck Panels Using Damage Plasticity Model. *Int. J. Concr. Struct. Mater.* **2015**, *9*, 45–54.
10. Tzaros, K.A.; Mistakidis, E.S.; Perdikaris, P.C. A numerical model based on nonconvex–nonsmooth optimization for the simulation of bending tests on composite slabs with profiled steel sheeting. *Eng. Struct.* **2010**, *32*, 843–853.
11. Gholamhoseini, A.; Gilbert, R.; Bradford, M.; Chang, Z. Longitudinal shear stress and bond–slip relationships in composite concrete slabs. *Eng. Struct.* **2014**, *69*, 37–48, doi:10.1016/j.engstruct.2014.03.008.
12. Clement, T.; Ramos, A.P.; Ruiz, M.F.; Muttoni, A. Design for punching of prestressed concrete slabs. *Structural Concrete* **2013**, 14(2), 157-167, doi: 10.1002/suco.201200028. https://doi.org/10.1002/suco.201200028
13. Van Greunen, J.; Scordelis, A.C. Nonlinear analysis of prestressed concrete slabs. *Journal of Structural Engineering* **1983**, 109, 1742-1760.
14. da Silva, A.R.; de Souza Rosa, J.P. Nonlinear numerical analysis of prestressed concrete beams and slabs. *Engineering Structures* **2020**, 223, 111187. https://doi.org/10.1016/j.engstruct.2020.111187
15. Sathurappan, G.; Rajogopalan, N.; Krishnamoorthy, C.S. Nonlinear finite element analysis of reinforced and prestressed concrete slabs with reinforcement (inclusive of prestressing steel) modelled as discrete integral components. *Computers & Structures* **1992**, 44(3), 575-584. https://doi.org/10.1016/0045-7949(92)90390-L
16. Buannic, N.; Cartraud, P.; Quesnel, T. Homogenization of corrugated core sandwich panels. *Compos. Struct.* **2003**, *59*, 299–312. https://doi.org/10.1016/S0263-8223(02)00246-5.
17. Terada, K.; Kikuchi, N. Nonlinear homogenization method for practical applications. *American Society of Mechanical Engineers, Applied Mechanics Division, AMD* **1995**, 212, 1-16.
18. Xin, L.; Khizar, R.; Peng, B.; Wenbin, Y. Two-Step Homogenization of Textile Composites Using Mechanics of Structure Genome. *Compos. Struct*, **2017**, *171*, 252–262, doi:10.1016/j.compstruct.2017.03.029.
19. Garbowski, T.; Marek, A. Homogenization of corrugated boards through inverse analysis. In Proceedings of the 1st International Conference on Engineering and Applied Sciences Optimization, Kos Island, Greece, 4–6 June 2014; pp. 1751–1766.
20. Hohe, J. A direct homogenization approach for determination of the stiffness matrix for microheterogeneous plates with application to sandwich panels. *Compos. Part. B* **2003**, *34*, 615–626.
21. Biancolini, M.E. Evaluation of equivalent stiffness properties of corrugated board. *Comp. Struct.* **2005**, *69*, 322–328.
22. Garbowski, T.; Gajewski, T. Determination of transverse shear stiffness of sandwich panels with a corrugated core by numerical homogenization. *Materials* **2021**, *14*, 1976, doi:10.3390/ma14081976.

23. Sotiropoulos, S.; Kazakis, G.; Lagaros, N. D. Conceptual design of structural systems based on topology optimization and prefabricated components. *Computers & Structures* **2020**, *226*, 106136.
24. Lian, Y.; Uzzaman, A.; Lim, J.B.; Abdelal, G.; Nash, D.; Young, B. Effect of web holes on web crippling strength of cold-formed steel channel sections under end-one-flange loading condition–Part I: Tests and finite element analysis. *Thin-Walled Struct.* **2016**, *107*, 443–452. https://doi.org/10.1016/j.tws.2016.06.025.
25. Parastesh, H.; Hajirasouliha, I.; Taji, H.; Sabbagh, A.B. Shape optimization of cold-formed steel beam-columns with practical and manufacturing constraints. *J. Constr. Steel Res.* **2019**, *155*, 249–259. https://doi.org/10.1016/j.jcsr.2018.12.031.
26. Sojobi,A,O.; Liew, K.M. Multi-objective optimization of high performance bio-inspired prefabricated composites for sustainable and resilient construction. *Composite Structures* **2022**, 279, 114732, https://doi.org/10.1016/j.compstruct.2021.114732.
27. Xiao, Y., Bhola, J. Design and optimization of prefabricated building system based on BIM technology. *International Journal of System Assurance Engineering and Management* **2022**, *13*, 111–120. https://doi.org/10.1007/s13198-021-01288-4
28. Xie, L.; Chen, Y.; Chang, R. Scheduling optimization of prefabricated construction projects by genetic algorithm. *Applied Sciences* **2021**, 11(12), 5531. https://doi.org/10.3390/app11125531
29. Staszak, N.; Garbowski, T.; Ksit, B. Optimal Design of Bubble Deck Concrete Slabs: Sensitivity Analysis and Numerical Homogenization. *Materials* **2023**, 16, 2320. https://doi.org/10.3390/ ma16062320
30. Staszak, N.; Garbowski, T.; Szymczak-Graczyk, A. Solid Truss to Shell Numerical Homogenization of Prefabricated Composite Slabs. *Materials* **2021**, *14*, 4120. https://doi.org/10.3390/ma14154120.
31. Reich, E.V.; Lima, M.; Strelets, K.I. Efficiency of Applying Sustainable Technology of Bubbledeck Technology in Concrete in Russia. *Construction of Unique Buildings and Structures* **2017**, 11(62), 83-92.
32. Shetkar, A.; Hanche, N. An Experimental Study on Bubble Deck Slab System with Elliptical Balls. In *Proceeding of NCRIET-2015 & Indian Journal of Scientific Research* **2015**, 12(1), 21–27.
33. Hokrane, N.S.; Saha, S. Comparative Studies of Conventional Slab and Bubble Deck Slab Based on Stiffness and Economy. *International Journal for Scientific Research & Development* **2017**, 5(3), 1396 – 1398.
34. Fuchs, A.C. BubbleDeck Floor System – An Innovative Sustainable Floor System. BubbleDeck Netherlands B.V., AD Leiden, the Netherlands, **2009**.
35. Jamal, J.; Jolly, J. A study on structural behaviour of bubble deck slab using spherical and elliptical balls. *International Research Journal of Engineering and Technology* **2017**, 4(5), 2090– 20957.
36. Konuri, S.; Varalakshmi, T.V.S. Review on Bubble Deck Slabs Technology and their Applications. *International Journal of Scientific and Technology Research* **2019**, 8(10), 427–432.
37. Kyng Consulting PTY Ltd, "BubbleDeck Design Guide for Compliance with BCA Using AS3600 and EC2," BubbleDeck Australia and New Zealand, DG-V.1.2, 2008.
38. PN-EN 1992-1-1:2008 - Eurocode 2: Design of concrete structures - Part 1-1: General rules, and rules for buildings, 2008.
39. PN-EN 1990:2004 – Eurocode 0: Basics of structural design, 2004.
40. Garbowski, T.; Knitter-Piątkowska, A.; Mrówczyński, D. Numerical Homogenization of Multi-Layered Corrugated Cardboard with Creasing or Perforation. *Materials* **2021**, 14, 3786. https:// doi.org/10.3390/ma14143786
41. Mrówczyński, D.; Knitter-Piątkowska, A.; Garbowski, T. Non-Local Sensitivity Analysis and Numerical Homogenization in Optimal Design of Single-Wall Corrugated Board Packaging. *Materials* **2022**, 15, 720. https://doi.org/10.3390/ma15030720
42. Mrówczyński, D.; Knitter-Piątkowska, A.; Garbowski, T. Numerical Homogenization of Single-Walled Corrugated Board with Imperfections. Appl. Sci. 2022, 12, 9632. https://doi.org/10.3390/ app12199632
43. Staszak, N.; Szymczak-Graczyk, A.; Garbowski, T. Elastic Analysis of Three-Layer Concrete Slab Based on Numerical Homogenization with an Analytical Shear Correction Factor. Appl. Sci. 2022, 12, 9918. https://doi.org/ 10.3390/app12199918
44. Reddy, J. N., Theory and analysis of elastic plates and shells, CRC Press, Taylor and Francis, 2007.
45. Timoshenko, S.; Woinowsky-Krieger, S., Theory of plates and shells, McGraw-Hill New York, 1959.
46. Software Version 2022a, Mathworks, Natick, Massachusetts, USA
47. Biggs, M.C. Constrained minimization using recursive quadratic programming. In Towards Global Optimization, North-Holland, Amsterdam, 1975.
48. Han, S.P. A globally convergent method for nonlinear programming. *J. Optim. Theory Appl.* **1977**, *22*, 297–309. https://doi.org/10.1007/bf00932858.
49. Powell, M.J.D. The convergence of variable metric methods for nonlinearly constrained optimization calculations. In proceedings of the Special Interest Group on Mathematical Programming Symposium Conducted by the Computer Sciences Department at the University of Wisconsin–Madison, July 11–13, 1977. https://doi.org/10.1016/b978-0-12-468660-1.50007-4.
50. Powell, M.J.D. A fast algorithm for nonlinearly constrained optimization calculations. *Numer. Anal.* **1978**, *630*, 144–157.
51. Nocedal, J.; Wright, S.J. *Numerical Optimization*, 2nd ed.; Springer Series in Operations Research; Springer: Berlin/Heidelberg, Germany, 2006.
52. Gajewski, T.; Staszak, N.; Garbowski, T., Parametric optimization of thin-walled 3D beams with perforation based on homogenization and soft computing. Materials 2022, 15, 2520. doi.org/10.3390/ma15072520